Postreceptoral chromatic detection mechanisms revealed by noise masking in three-dimensional cone contrast space

Marcel J. Sankeralli and Kathy T. Mullen

McGill Vision Research, Department of Ophthalmology, McGill University, 687 Pine Avenue West (H4-14), Montreal, Quebec H3A 1A1, Canada

Received December 2, 1996; revised manuscript received April 7, 1997; accepted April 15, 1997

We used a noise masking technique to test the hypothesis that detection is subserved by only two chromatic postreceptoral mechanisms (red–green and blue–yellow) and one achromatic (luminance) mechanism. The task was to detect a 1-c/deg Gaussian enveloped grating presented in a mask of static, spatially low-passed binary or Gaussian distributed noise. In the main experiment, the direction of the test stimulus (termed the signal) was constant in cone contrast space, and the direction of the noise was sampled in equally spaced directions within a plane (the noise plane) in the space. The signal was chosen to coincide with one of the three cardinal directions of three postulated mechanisms. The noise plane was selected to span two of the cardinal directions, including that chosen as the signal direction. As the noise direction was sampled around the noise plane, the signal detection threshold was found to vary in accordance with a linear cosine model, which predicted noise directions yielding maximum and minimum masking of the signal. In the direction of minimum masking (termed a null direction), the noise was found to have no masking effect on the signal. Moreover, the null was not orthogonal to the signal direction but lay instead in one of the cardinal directions. Our findings suggest that detection is mediated by only three mechanisms. In a further experiment we found little or no cross masking between each pair of cardinal directions up to the limit of our noise mask contrasts. This further supports the presence of no more than three independent postreceptoral mechanisms. © 1997 Optical Society of America [S0740-3232(97)02810-X]

1. INTRODUCTION

There is an ongoing controversy concerning the number of postreceptoral chromatic mechanisms subserving detection. Kranda and King-Smith[1] found that threshold contours based on three selected color primaries could be modeled by four postreceptoral mechanisms but not three. Krauskopf *et al.*[2] identified three cardinal directions (termed red–green, blue–yellow and luminance), where adaptation in any one direction did not raise detection threshold in another. However, a more detailed analysis of these and other data suggested the presence of further higher-order mechanisms.[3] Another study[4] found that color discrimination in the isoluminant plane was limited primarily to three cardinal axes, although higher-order mechanisms were also postulated. Noise-masking techniques have also been used to investigate postreceptoral chromatic mechanisms. One such study[5] supported the existence of two chromatic mechanisms, whereas another[6] suggested the presence of a greater number of chromatic detection mechanisms. More recently, preliminary studies in the (L, M) plane by Giulianini and co-workers[7,8] revealed red–green and luminance mechanisms from noise masking.

Based on the assumption that each mechanism results from a linear combination of the three cone types,[1,9,10] many studies have measured detection threshold contours in cone contrast space to investigate the detection mechanisms. Noorlander and Koenderink[11] used a three-mechanism model to describe elliptical fits to threshold contours in cone contrast space. Cole *et al.*[12] used a three-mechanism probability summation model[13] to estimate the relative cone weights to each mechanism. These estimates supported those of Stromeyer *et al.*[14] for the luminance and the red–green mechanisms. Sankeralli and Mullen[15] obtained similar estimates from superellipsoidal fits. These studies that use cone contrast space support the existence of at least three mechanisms: (i) a red–green mechanism consisting of equally opponent inputs from long-wavelength-sensitive (L) and middle-wavelength-sensitive (M) cones, (ii) a blue–yellow mechanism having inputs from short-wavelength-sensitive (S) cones balanced by some combination of L- and M-cone inputs, and (iii) a luminance mechanism consisting of additive L- and M-cone inputs with a higher contribution from L cones.

These methods do not test, however, whether these mechanisms alone subserve detection. Although detection threshold contours reliably reveal the most sensitive mechanisms (notably the red–green mechanism) under a given spatiotemporal condition, they cannot produce consistent estimates of less sensitive mechanisms. Specifically, the L- and M-cone inputs to the blue–yellow mechanism have not been established, and there is still divergence of estimated ratios of L- and M-cone inputs to the luminance mechanism, even considering the variability of the ratio with viewing conditions and subjects.[16] There is an inherent uncertainty in threshold contour methods, which arises from two principal causes. First, the model used to fit threshold contours assumes a particular number of mechanisms. The actual number of

0740-3232/97/1002633-14$10.00

mechanisms can thus be inferred only by comparison among such models and cannot be determined directly. Second, certain contours cannot be used to determine a unique set of underlying mechanisms. Specifically, unique underlying mechanisms cannot be derived from ellipsoidal fits.[17] Whether ellipsoidal fits are a suitable model of detection contours is still controversial. Although probability summation and superellipsoidal models provide a better chi-squared fit to threshold data,[15,18] the ellipsoidal model, taken as a null hypothesis, cannot be rejected in favor of these alternative models by F-tests and other statistical methods.[19]

A third critical issue in determining the number of postreceptoral mechanisms is the independence of these mechanisms. Independence here is defined as the condition in which the response of one mechanism does not depend on the responses of the other mechanisms; it is the underpinning of mechanism estimation with the use of threshold contours. Independence of the red–green and luminance mechanisms has been observed in adaptation experiments[2] and from measurements of noise-masking functions.[6,20] Studies that use a probability summation model[13] also support the independence of these mechanisms at detection threshold,[12,21] but another study that demonstrates linear summation contradicts mechanism independence.[22] Thus in attempting to reveal the number of underlying mechanisms from detection thresholds, it is important to establish whether these mechanisms are truly independent.

Finally, there is a previous study, using methods similar to our own, that contradicts the idea that only three postreceptoral mechanisms exist. From measurement of chromatic tuning functions in noise in the red–green/luminance plane, Gegenfurtner and Kiper[6] postulated the presence of additional mechanisms intermediate to those of red–green and luminance. This opposes the three-mechanism model, which purports only two mechanisms (luminance and red–green) in the red–green/luminance plane. We argue, however, that the interpretation of their data is critically dependent on the choice and scaling of the color axes. Gegenfurtner and Kiper[6] used an arbitrarily scaled color space whose axes corresponded to the cardinal axes of postreceptoral mechanisms observed by Krauskopf *et al.*[2] This choice of axes obscures the predictions of detection thresholds in noise, because models of detection are rooted at the level of cone combination. Instead, the most convenient color space representation for this analysis should reflect an underlying model of detection based on the cone responses.

In our study we used three-dimensional (L, M, S) cone contrast space to test whether the detection thresholds of test stimuli in the presence of noise could be accounted for by only three postreceptoral mechanisms. The cone weights to these three mechanisms (termed red–green, blue–yellow, and luminance) were selected from a previous study,[15] but our method permitted us to verify whether this selection was suitable. We measured detection threshold of a test stimulus (the signal) in the presence of visual noise.[23–25] The introduction of noise allowed us to observe the less sensitive mechanisms by masking the more sensitive mechanisms. Using these experiments we demonstrated that the signal threshold as a function of noise direction in color space could be fitted by a cosine model in cone contrast space. The model assumes a linear response of a mechanism to a particular stimulus and has been used in previous threshold contour studies.[12,14,15,21] Its application assumes the presence of a single mechanism that detects the signal, and the model can therefore be used to test for cases of detection by a single mechanism and to reveal the direction of that mechanism in cone contrast space. By showing systematically the cases in which the cosine model is obeyed, we demonstrate that our detection data can be accounted for by three mechanisms in our postulated directions. Two further control experiments were performed. In the first control, we verified the previously observed linear relationship[5,6,25,26] between signal threshold energy and noise power spectral density for stimuli in the (L, M) plane. In the second control, we demonstrated the independence of our three purported mechanisms by placing signal and noise in their cardinal directions. In a final experiment, we used noise analysis to estimate the L- and M-cone inputs to the blue–yellow mechanism, for which there are few data and no consensus from earlier studies.

2. METHODS

A. Apparatus

The stimuli were presented on a Barco Calibrator CCID7651 RGB monitor driven by a Cambridge Research Systems VSG2/1 video controller interfaced with a Dell 333D computer. The monitor was set at a line rate of 60 kHz, a frame rate of 75 Hz, and a pixel resolution of 672×750. The screen had a mean luminance of $55\ \mathrm{cd\ m^{-2}}$ near the equal-energy white point [CIE (0.28, 0.30)]. It was viewed at 1.5 m, subtending an angle of $11° \times 11°$. The monitor phosphors were driven by a 14-bit digital-to-analog converter fed by 12-to-14-bit lookup tables. Each phosphor output was linearized by use of a gamma correction[27] and a second-stage linear fit made from irradiance measurements by use of a United Detector Technology Optometer (UDT S370) fitted with a radiometric detector (Model 260). The contrast error in each phosphor was less than 0.017 log unit.

B. Stimuli

The stimulus consisted of a 1-c/deg sinusoidal grating (the signal) embedded in additive, static, one-dimensional, low-pass-filtered white noise. Both the grating and the noise were horizontally oriented, spatiotemporally Gaussian enveloped. The noise was of one of two types, both of which were flat in the spatial passband determined by low-pass filtering and thus, for a linear model, differed in effect only by the magnitude of masking produced. The first type, used in the first control experiment only, was low-passed Gaussian noise, in which the pixelwise (in this case, linewise) contrast before low-pass filtering was drawn randomly[28] from a Gaussian distribution (truncated at ± 2 standard deviation) centered on zero contrast (i.e., the background state). In all other experiments, low-passed binary noise was used in which the linewise contrast before low-pass filtering was selected randomly[28] from two values whose mean again was at zero contrast. The noise contrast C_n provides a measure of the noise en-

ergy ($\alpha {C_n}^2$). For low-passed Gaussian noise, C_n was quoted as the standard deviation of the Gaussian distribution of the prefiltered linewise contrast; for low-passed binary noise, it was quoted as the two allowable values ($\pm C_n$) of this contrast. Spatial low-pass filtering was used in all experiments to remove artifacts resulting from chromatic aberration[29,30] and was achieved by using an IIR fourth-order (160 dB/decade roll-off) Type II Chebyshev filter[31] with a 40-dB cutoff at 4 c/deg. Both the grating and the noise were modulated in the vertical direction only. In this direction both grating and noise were Gaussian enveloped ($\sigma = 1.4°$). In the horizontal direction, grating and noise were hard-edged windowed in a strip (width = 4°) at the center of the screen. On either side of the window the screen was fixed at the background state. The stimulus was also temporally Gaussian enveloped ($\sigma = 88$ ms). The spatial and temporal Gaussian envelopes were used to restrict the spatiotemporal bandwidths of the stimuli and to maintain the mean luminance and chromaticity over space and time at the background state.

Signal and noise were represented in a three-dimensional cone contrast space. Each axis represented the quantal catch of the L-, M-, and S-cone types normalized with respect to the white background.[11] The required phosphor contrasts were calculated from these three cone contrasts by a linear transformation.[15] Signal and noise were represented in a spherical (R, θ, ϕ) system, where R, the stimulus contrast, and (θ, ϕ), the stimulus direction, were given by

$$R = (L^2 + M^2 + S^2)^{1/2};$$

$$\theta = \sin^{-1}\left[\frac{M}{(L^2 + M^2)^{1/2}}\right];$$

$$\phi = \sin^{-1}\left[\frac{S}{(L^2 + M^2 + S^2)^{1/2}}\right]. \quad (1)$$

Signal and noise directions were alternatively represented by a Cartesian vector $[aL + bM + cS]$. The postreceptoral mechanisms were also represented in this space as vectors in the direction of maximum mechanism sensitivity. The L, M, S ratios of these vectors corresponded to the relative effective cone weights to the mechanism at that spatiotemporal condition.[11,12]

Since we are testing the predictions of a three-mechanism model, we derive three cardinal stimulus directions in cone contrast space that can be used to stimulate each of the purported mechanisms uniquely. These cardinal directions are therefore analogous to those used to probe higher-order color mechanisms (e.g., Krauskopf *et al.*[2]), as they can each be used to probe a single postreceptoral mechanism. Each cardinal direction is obtained by seeking the direction in which a stimulus is invisible to all but one mechanism, regardless of whether that mechanism is optimally stimulated. For linear mechanisms in cone contrast space, the cardinal direction of a given mechanism is given by the unique direction orthogonal to the two vectors that represent the other two mechanisms and is calculated, therefore, as the cross product of those two vectors. Therefore each cardinal direction does not correspond directly to its associated mechanism direction, nor are the cardinal directions orthogonal to one another in cone contrast space. In our previous study[15] we estimated the red–green, blue–yellow, and luminance mechanism directions to be approximately L − M, S − (L + M)/2, and 3L + M. Using these directions, our calculated cardinal directions are L − 3M − S, S, and L + M + S, respectively. For all but the red–green direction, these correspond to the axes of the cardinal color space proposed by MacLeod and Boynton.[32]

C. Procedure

In each trial of a two-alternative–forced-choice paradigm, a signal + noise stimulus and a noise-only stimulus were presented in random order in two consecutive 500-ms intervals, each signaled by a tone. All experiments were performed monocularly with natural viewing. The noise was identical in the two frames. The object of each trial was to detect the stimulus containing the signal, which the subject reported by button press. Audio feedback was provided. Two procedures were used, both yielding an 81.6% correct detection level. Unless otherwise stated in the text, a staircase procedure was used, in which detection thresholds were obtained by averaging the last six reversals.[15] Alternatively, a QUEST procedure was used, where the threshold was estimated from 45 trials.[33] For each procedure the average of at least three threshold measurements was obtained.

D. Observers

The two authors and one naïve observer acted as subjects in these experiments. Observers wore their usual optical corrections and tested normally on the Farnsworth–Munsell 100-hue color test.

3. RESULTS

A. Control Experiment 1: Linearity of Signal Energy versus Noise Power Spectral Density

In order to use noise masking quantitatively, we first determined the variation of signal threshold with noise contrast for several fixed signal and noise directions. Earlier results[6,25,26] demonstrated a linear relationship between signal energy threshold E with noise power spectral density N:

$$E = kN + E_0, \quad (2)$$

where E_0 is the signal threshold energy in the absence of noise and k is related to the sampling efficiency η by the relationship

$$k = \frac{d'^2}{\eta}, \quad (3)$$

where d' is the signal-to-noise ratio at detection threshold for an ideal observer. Since E is proportional to the signal contrast threshold squared ${C_s}^2$ and N is proportional to the noise contrast squared ${C_n}^2$, this relationship can be rewritten as

$${C_s}^2 = \frac{1}{J}{C_n}^2 + {C_0}^2, \quad (4)$$

where C_0 is the signal contrast threshold in the absence of noise and J is proportional to the sampling efficiency η.

In our experiment the signal and the noise were confined to the (L, M) plane. The signal was placed in one of four directions: $\theta = +45°$ (L + M: ~luminance), $\theta = -45°$ (L − M: ~red–green), $\theta = 0°$ (L-cone direction: light red/dark green), and $\theta = 90°$ (M-cone direction: dark red/light green). For each signal direction the noise was placed in the same direction (the self condition) or in the orthogonal direction (the cross condition). Our results are shown in Fig. 1 (self condition) and Fig. 2 (cross condition) for the one subject tested. Signal threshold squared (C_s^2) is plotted as a function of noise contrast squared (C_n^2) on log–log coordinates. These noise-masking functions were fitted to the linear model of Eq. (4), with the resulting fit parameters given in Table 1. The masking functions obtained obeyed the linear relationship in both the self and the cross conditions.

The result of this relationship is that, for $C_n \gg C_0$ in Eq. (4),

$$C_s \cong \frac{1}{\sqrt{J}} C_n . \tag{5}$$

This means that for effective noise masks, signal threshold C_s varies linearly with noise contrast C_n. Coupled with the assumption of linearity of cone inputs to postreceptoral mechanisms, this sets up the cosine model used in the main experiment. However, the cosine model also depends on the mutual independence of the postreceptoral mechanisms, as tested for in the following control experiment.

B. Control Experiment 2: Independence of Cardinal Directions

In this experiment we tested the independence of the three postulated mechanisms for two subjects by placing the signal and noise in the cardinal directions of each of the three mechanisms. All nine pairwise combinations of cardinal directions for signal and noise were tested. For each combination the signal threshold was measured as a function of the noise contrast squared as in control experiment 1.

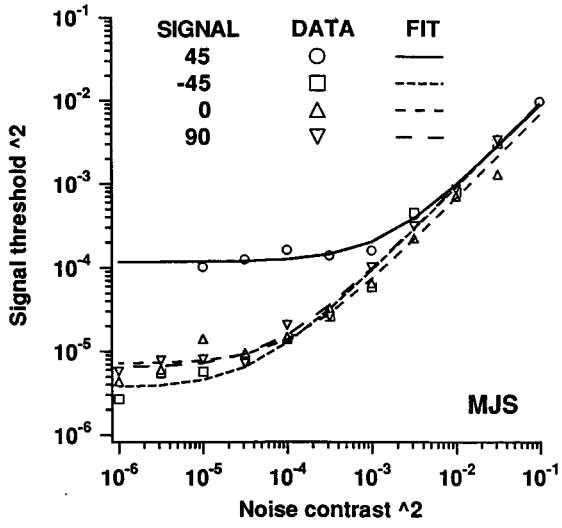

Fig. 1. Signal threshold versus noise contrast: self condition. Signal versus noise functions plotted for four signal directions in the (L, M) plane (legend), with noise fixed in same direction as signal. Curves represent fits to linear model (Table 1). Standard errors in signal threshold squared are approximately 0.1 log unit.

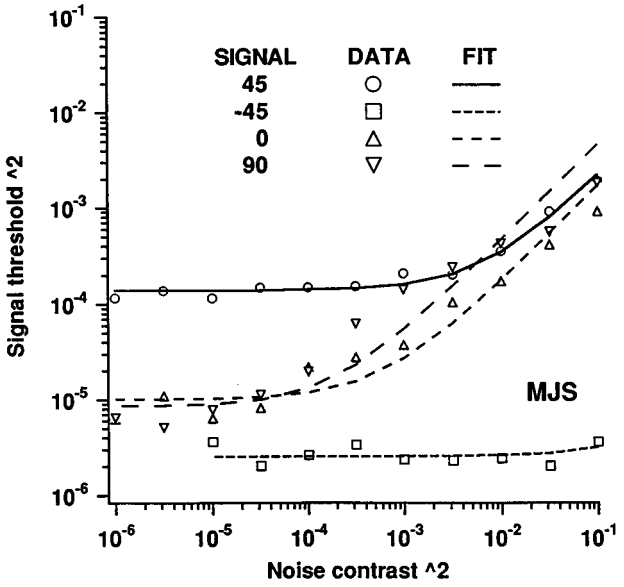

Fig. 2. Signal threshold versus noise contrast: cross condition. Signal versus noise functions plotted for four signal directions in the (L, M) plane (legend), with noise fixed in the direction orthogonal to that of the signal. Curves represent fit to the linear model (Table 1). Standard errors in signal threshold squared are approximately 0.1 log unit.

Table 1. Fitted Values of Scaled Efficiency J and Signal Contrast Threshold C_0 for Self and Cross Conditions[a]

	SELF		CROSS	
Signal (deg)	J	C_0 (%)	J	C_0 (%)
45	11.78	1.08	48.31	1.18
−45	11.16	0.19	1.5×10^5	0.16
0	15.03	0.27	59.52	0.32
90	10.90	0.25	21.68	0.29

[a] Fits of data (Figs. 1 and 2) to linear model $C_s^2 = 1/JC_n^2 + C_0^2$, where C_s and C_n are signal contrast threshold and noise contrast respectively. C_0 is therefore equal to the signal threshold in the absence of noise (expressed as percent cone contrast).

The masking functions are plotted on a log–log scale in Fig. 3. Each panel shows the masking functions for the three noise directions corresponding to a given signal direction. The results show that in the three cases in which the signal is in the same direction as the noise (subject MJS only), the masking functions are similar to those obtained in the self condition in the first control experiment. When the signal and noise are not in the same cardinal direction (both subjects), the masking function is flat. The flat masking function indicates that the noise has no effect on signal detection within the range of noise magnitudes attainable. There is, however, noticeable facilitation for near-threshold noise contrasts, especially for the luminance signal, and a small degree of masking at suprathreshold noise contrasts. The latter may result from cross-mechanism interactions at high contrast or be

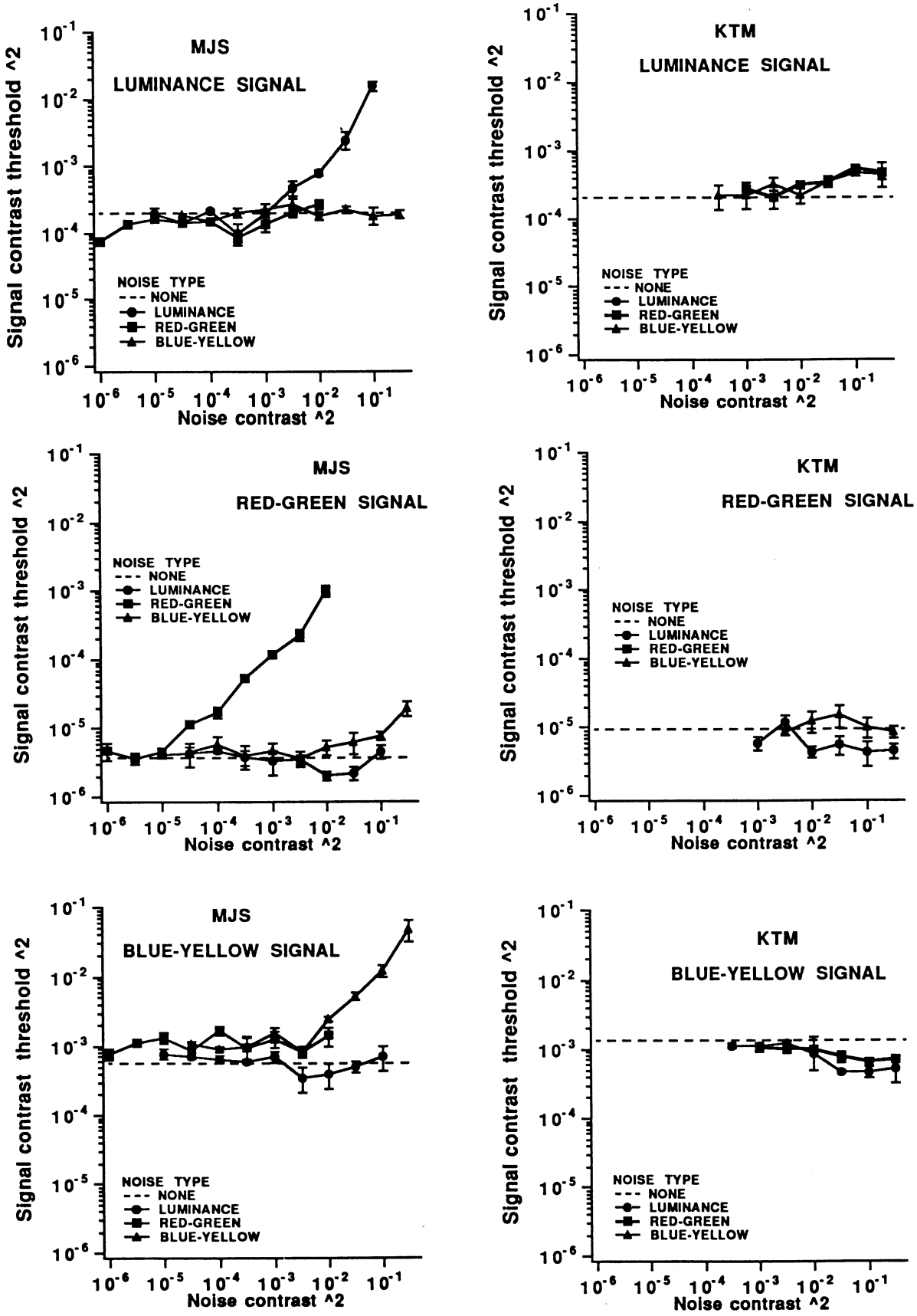

Fig. 3. Masking functions in cardinal directions. Signal versus noise-masking functions obtained for signal and noise placed in each of our three cardinal directions (legend). Masking of signal and noise in different cardinal directions is much less than for signal and noise in the same direction. A small facilitation is observed for near-threshold luminance noise.

due to small errors in the selection of the cardinal directions. Our results nonetheless suggest that the underlying detection mechanisms are all independent within our range of noise contrast.

C. Main Experiment: Chromatic Tuning Functions

We tested whether detection is subserved by three postreceptoral mechanisms that are based on linear cone combinations by measuring the variation of signal threshold with noise direction in three-dimensional cone contrast space. In each test condition the signal was placed in a fixed direction (the signal direction), and the noise direction was varied within a preselected plane (the noise plane) in this space. Three signal directions were used, one in each of the cardinal directions, termed the red–green (rg), blue–yellow (by), and luminance (lum) directions. Three noise planes were used, one spanning each pair of cardinal directions, and were termed the blue–yellow/luminance (by/lum), red–green/luminance (rg/lum) and red–green/blue–yellow (rg/by) planes. In each condition the signal direction was fixed and the noise was placed at a fixed contrast in one of 12 equally spaced directions (the noise direction) in the noise plane. For each noise plane, the noise contrast was fixed in cone contrast space. This was necessary for the direct application of the cosine model. The fixed noise contrast for each noise plane (10% for the rg/lum and rg/by planes and 40% for the by/lum plane) was selected as the highest value that fulfilled this condition. The signal detection threshold was measured for each of the noise directions. Six conditions are shown in Figs. 4–9. These comprise five conditions in which the signal was in one of the three cardinal directions and one condition in which the signal was in an intermediate direction. In each figure the signal direction and the noise plane are illustrated in the top-left panel. The results for the three subjects are shown in the remaining panels.

1. *rg* Signal Presented in *rg*/*by* Noise

The results in this condition are shown in Fig. 4. The signal was fixed in the red–green cardinal direction, while the noise was varied in the plane containing the red–green and blue–yellow cardinal directions. Because the red–green and the blue–yellow cardinal axes are both orthogonal to the purported luminance mechanism, this noise plane is the purported isoluminant plane. Note however that because our plot is in cone contrast space, the cardinal directions are not orthogonal. In this, as in all other plots, the axes were chosen as the most convenient pair of orthogonal axes in the plane. The axes of

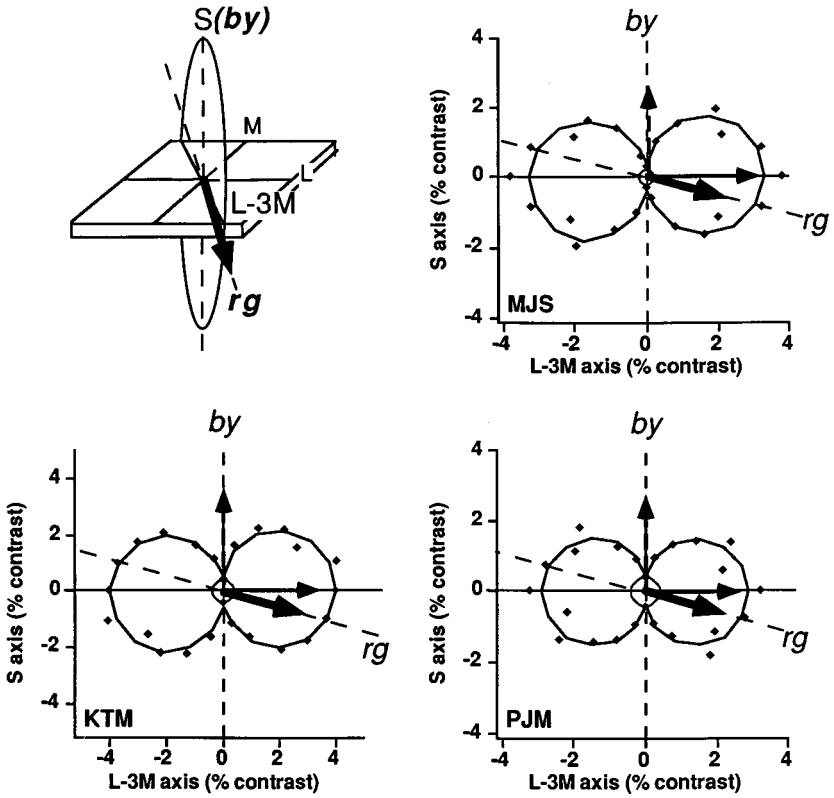

Fig. 4. *rg* signal in *rg*/*by* noise. Top left, fixed signal direction (thick arrow) and noise plane (circle) in (L, M, S) cone contrast space. Bold italic labels represent the cardinal directions spanning the plane; large solid labels represent the reference axes in the plane. Remaining panels, detection threshold of fixed signal (thick arrow) in the absence of noise (radius of inner circle) and as a function of noise direction in the plane (diamond data points). The direction of data points from the origin represents applied noise direction in the plane; distance from the origin represents cone contrast threshold. The average standard error for each data point is approximately one tenth of its radial distance from the origin. Maximum (thin solid arrow) and minimum (thin dashed arrow) signal thresholds are obtained by cosine fit (solid curve). The minimum threshold predicted from the three-mechanism model lies along one of the cardinal directions (dashed lines). Noise contrast is fixed at 10%. A null is found when noise is placed in the blue–yellow cardinal direction, confirming signal detection by the red–green mechanism and showing little S-cone input to this mechanism. Data points at null are obscured in the figure.

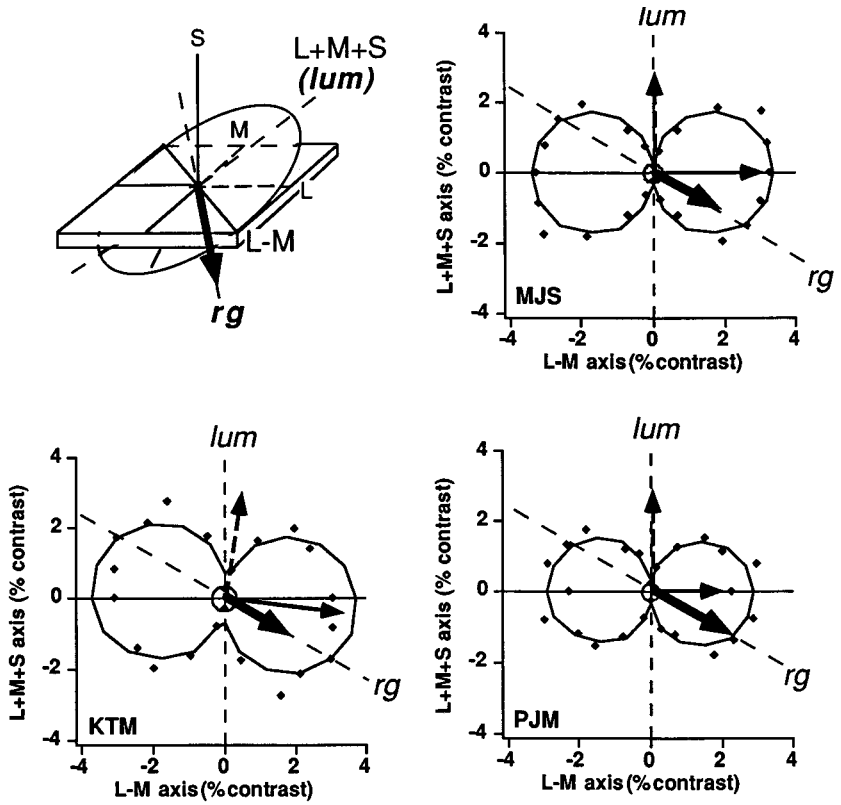

Fig. 5. *rg* signal in *rg*/*lum* noise. See caption for Fig. 4. Noise contrast is fixed at 10%. The direction of maximum masking confirms that the red–green mechanism lies in the L − M direction. Data points at null are obscured in the figure.

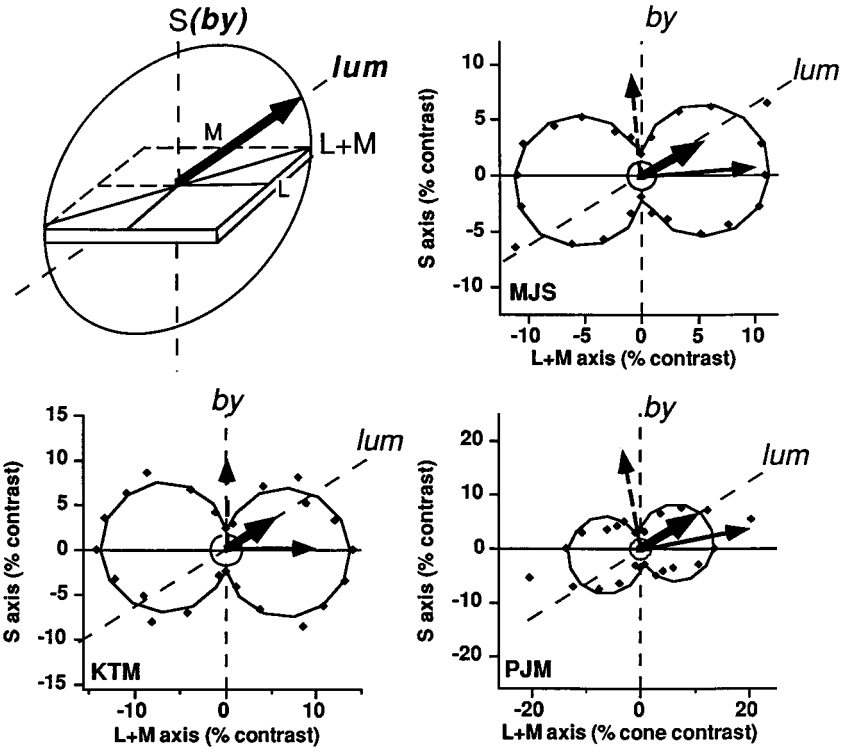

Fig. 6. *lum* signal in *by*/*lum* noise. See caption for Fig. 4. Noise contrast is fixed at 40%. Null in the blue–yellow cardinal direction confirms signal detection by the luminance mechanism. Deviation of the maximum masking direction from the L + M axis for two subjects, with small S-cone input to the luminance mechanism.

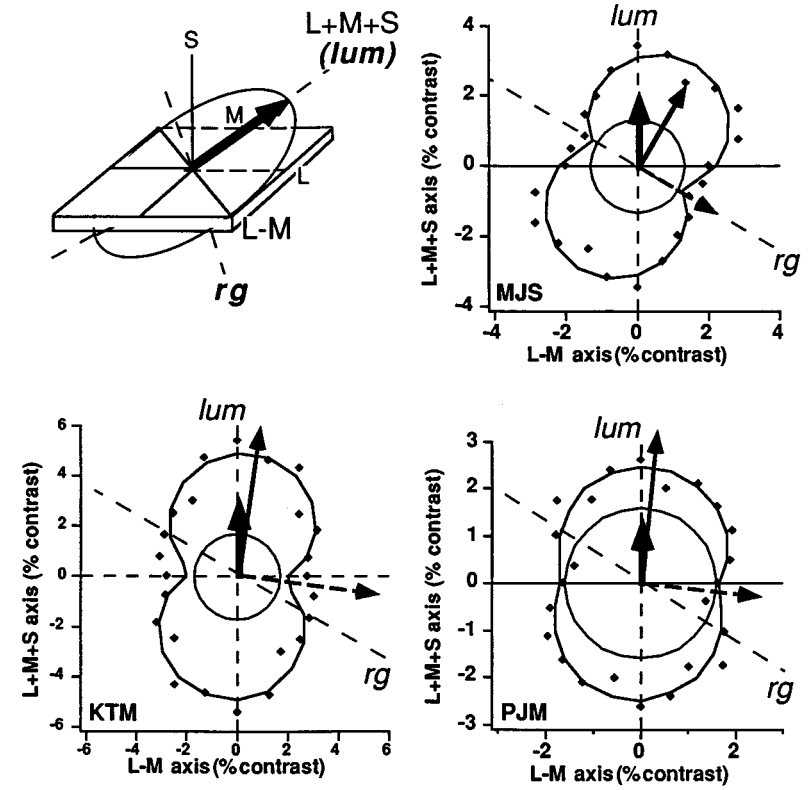

Fig. 7. *lum* signal in *rg*/*lum* noise. See caption for Fig. 4. Noise contrast is fixed at 10%.

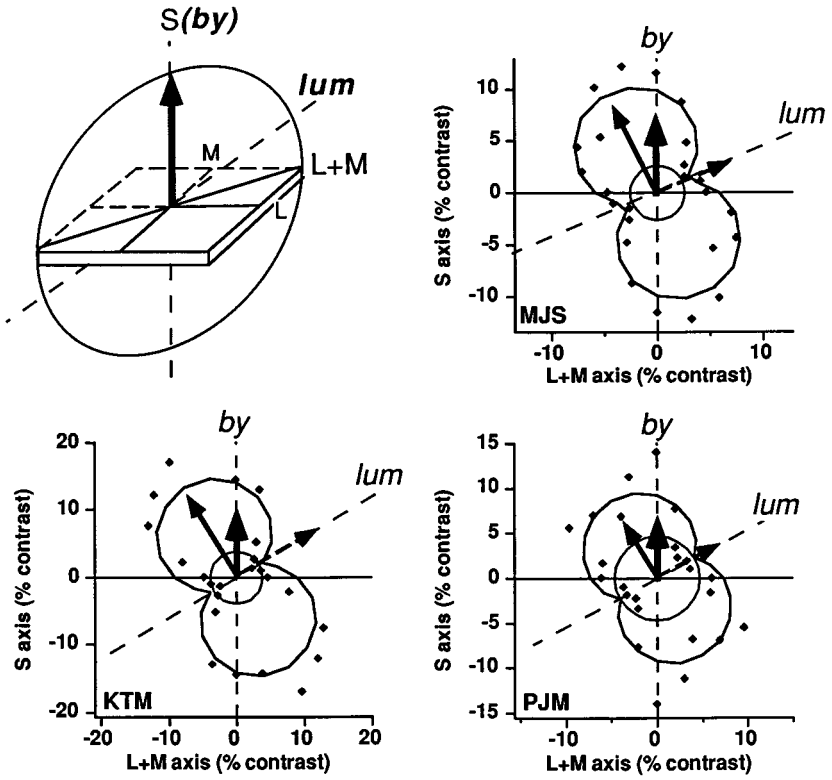

Fig. 8. *by* signal in *by*/*lum* noise. See caption for Fig. 4. Noise contrast is fixed at 40%. Null in the luminance cardinal direction confirms detection by the blue–yellow mechanism. The inward deviation of the data relative to the cosine model near the L+M axis suggests facilitation by luminance noise (Fig. 3).

this plane are the L − 3M and the S directions (the latter being the blue–yellow cardinal direction) and are scaled in units of cone contrast.

The signal was fixed in the red–green cardinal direction (thick solid arrow). Signal threshold was measured in the absence of noise (radius of inner circle) and then for each of 12 noise directions in the plane (diamonds). The noise contrast was fixed for all 12 directions at the maximum permissible constant level. Because of the symmetry in color space of the stimulus, the data points occur in pairs symmetric about the origin. The distance between each point and the inner circle represents the masking effect of the noise in that direction. As the noise direction is varied in the plane, the masking effect varies between a maximum (in this case near the horizontal axis) and a minimum occurring in the orthogonal direction. In the direction of minimum masking, the data point coincides with the inner circle—i.e., there is no masking effect. We call this a null condition. The presence of a null indicates that signal detection is subserved for all noise directions by a single mechanism. It is important to note that the null direction is not orthogonal to the fixed signal direction. Thus the null is not determined directly by the signal direction but by the direction of the single underlying mechanism.

The data were fitted by a cosine model (solid curve). The cosine model states that the masking effect is proportional to the cosine of the angle between the noise direction and that of the underlying mechanism. The model assumes (i) linear cone inputs to the postreceptoral mechanisms, (ii) a linear relationship between noise contrast and signal threshold (control experiment 1), (iii) independence of the postreceptoral mechanisms (control experiment 2), and (iv) a single mechanism underlying signal detection. A good fit to the data therefore supports the presence of only one mechanism detecting the signal in all cases. The model was of the form

$$R = R_0 + A \cos|\theta - \theta_0|, \tag{6}$$

where R is the signal threshold in noise (noise direction θ) relative to a reference axis, R_0 is the zero-noise signal threshold, A represents the maximum masking effect, and θ_0 represents the noise direction of maximum masking, which corresponds to the projection of the single underlying mechanism that detects the signal. The fit of A and θ_0 permitted precise estimation of the directions of maximum masking (thin solid arrow) and minimum masking (thin dashed arrow). For all three subjects, maximum masking does not occur in the signal direction, and, correspondingly, the minimum (null) direction is not orthogonal to the signal. From the cosine model, the direction of maximum masking yields the projection of the single underlying signal detection mechanism onto the plane. In this condition this projection lies near the horizontal axis, indicating that the underlying mechanism has little S-cone input. Furthermore, the three-mechanism model (i.e., two mechanisms in the chosen noise plane) predicts that the direction of minimum masking should correspond to the cardinal direction of a mechanism not involved in signal direction. For all three subjects the null is in the blue–yellow cardinal direction and thus in accordance with the presence of only three mechanisms.

2. rg Signal Presented in rg/lum Noise

These results are shown in Fig. 5. The signal is the red–green cardinal direction as in the previous condition. The noise plane, however, now passes through the red–green and luminance cardinal directions as shown. The axes of this plane were chosen to be the L + M + S (luminance cardinal direction) and the L − M directions. As before, the signal direction is shown by the thick solid arrow. The thin solid and the dashed arrows represent the noise directions of maximum and minimum masking, respectively. Again, for noise in the direction of minimum masking, the signal threshold in the presence of noise (diamonds) is near the signal threshold in the absence of noise (radius of inner dashed circle), yielding a null condition. Once more, the null is not orthogonal to the signal direction and thus appears to be determined by the direction of an underlying mechanism. From the cosine fit, the null was found to be near the luminance cardinal direction, as predicted by the presence of only three mechanisms. The mechanism projection is in the L − M direction. Given that we observed in the previous condition that this mechanism has little S-cone input, we conclude that the detection of the signal in the red–green cardinal direction is subserved by a mechanism with an L−M cone weight with little S-cone input.

3. lum Signal Presented in by/lum Noise

These results are shown in Fig. 6. In this condition, the signal (thick solid arrow) was fixed in the luminance cardinal direction. The noise plane passed through the blue–yellow and luminance cardinal directions. The L + M and S directions were chosen as the axes of this plane. The signal threshold (diamonds) in the direction of minimum masking (thin dashed arrow) is near the signal threshold in the absence of noise (radius of inner circle). Once more, this null direction is not orthogonal to the signal. The cosine fit reveals that the null is near the blue–yellow cardinal direction, as expected from a three-mechanism model. The mechanism projection lies slightly above the L + M axis. This demonstrates that the mechanism that subserves detection in the luminance cardinal direction has only a small S-cone input.

4. lum Signal Presented in rg/lum Noise

These results are shown in Fig. 7. The signal was fixed in the luminance cardinal direction as in the previous condition. The noise was varied in a plane spanning the red–green and luminance cardinal axes. In this condition, the results for the three subjects were different. For subject MJS the data were fitted by the a cosine rule, with a null in the red–green cardinal direction as predicted. We thus deduce for this subject that detection is served uniquely by a luminance mechanism in the purported direction. For subject KTM the minimum masking achieved did not create a null; and for subject PJM the maximum masking attained was weak. Both of these results suggest partial detection by a second mechanism in the plane, which is consistent with the high sensitivity of

the red–green mechanism relative to that for luminance in this spatiotemporal condition.

5. by Signal Presented in by/lm Noise

These results are shown in Fig. 8. The signal is in the blue–yellow cardinal direction. The noise plane passes through the blue–yellow and luminance cardinal directions. From the cosine fit, the null direction for all three subjects is in the luminance (L + M + S) cardinal direction, and maximum masking occurs in the S − (L + M)/2 direction. This confirms earlier results[15] that the S-cone and the combined L- and M-cone inputs to the blue–yellow mechanism are roughly balanced. We note that in this condition the cosine rule is not strictly obeyed. Notably, the data tend to lie within the predicted curve near the L + M axis. This may occur as a result of the facilitation of the blue–yellow mechanism (and perhaps of the red–green mechanism, which, owing to its high sensitivity, may also contribute to detection) by luminance noise, as observed in the second control experiment (Fig. 3).

6. Intermediate (L-cone) Signal Presented in rg/lum Noise

To test for the number of underlying mechanisms further, the signal was placed in a direction intermediate to the cardinal directions. This signal direction was chosen as the L-cone, or (0°, 0°), direction and the noise was varied in the red–green/luminance noise plane. The results are shown in Fig. 9. The cosine model is a poorer fit to the data than in previous conditions; specifically, there is maximum masking for all three subjects when the noise is closest to the signal direction. This may suggest the presence of a weaker intermediate mechanism tuned to the signal direction, as proposed by Gegenfurtner and Kiper,[6] or may reflect cues from differential phase shifts as proposed by Chaparro *et al.*[34] The null, defined as the data point closest to the circle representing zero-noise threshold, lies along the luminance cardinal axis for all three subjects and is not orthogonal to the signal direction. This demonstrates that the signal is detected primarily by the red–green mechanism and so is inconsistent with detection by an intermediate mechanism tuned to the signal direction. This suggests that the masking peak arises instead from cues that are due to differential phase shifts between the luminance and the red–green mechanisms that are likely to occur for noncardinal signal directions.

D. Estimate of the L- and M-cone Weights to the Blue–Yellow Mechanism

In each condition of the main experiment above, we determined the projection onto the given noise plane of the underlying mechanism. These projections can be used to estimate the mechanism directions and therefore the associated cone weights. In this experiment we estimated the L- and M-cone weights to the blue–yellow mechanism by the above approach. This estimate is difficult to obtain because of the overwhelming sensitivity of the red–green mechanism relative to the blue–yellow mechanism. We made a few adaptations to the main experiment to obtain this estimate. First, with the signal fixed in the

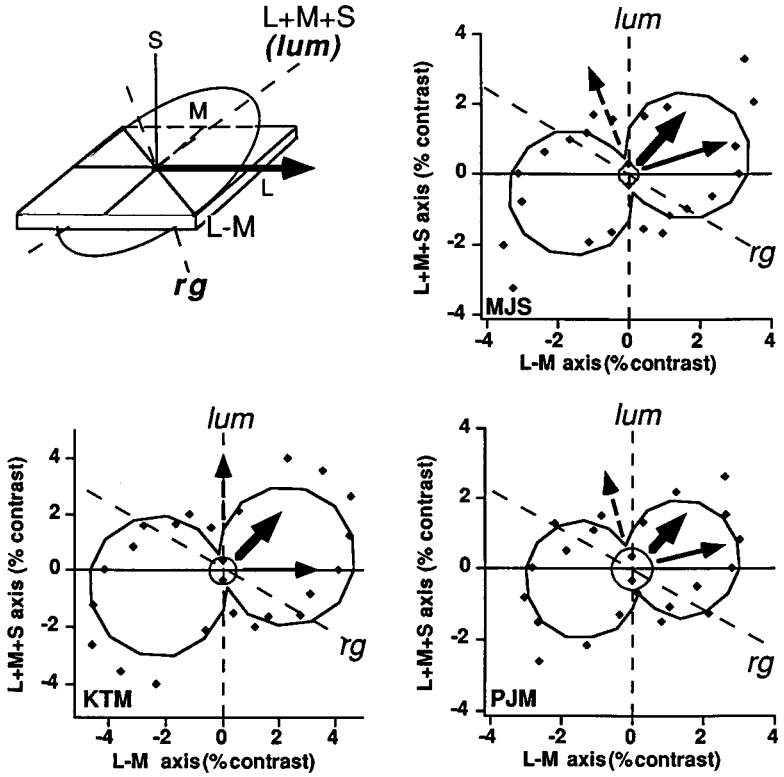

Fig. 9. Intermediate (L-cone) signal in *rg/lum* noise. See caption for Fig. 4. Noise contrast is fixed at 10%. For subject PJM, signal thresholds were measured by the QUEST procedure. Nulls lie in the luminance cardinal direction, indicating primary detection by the red–green mechanism (data points at null for subject MJS are obscured). However, systematic distortion with respect to the cosine model suggests the influence of the luminance mechanism (compare with Fig. 12).

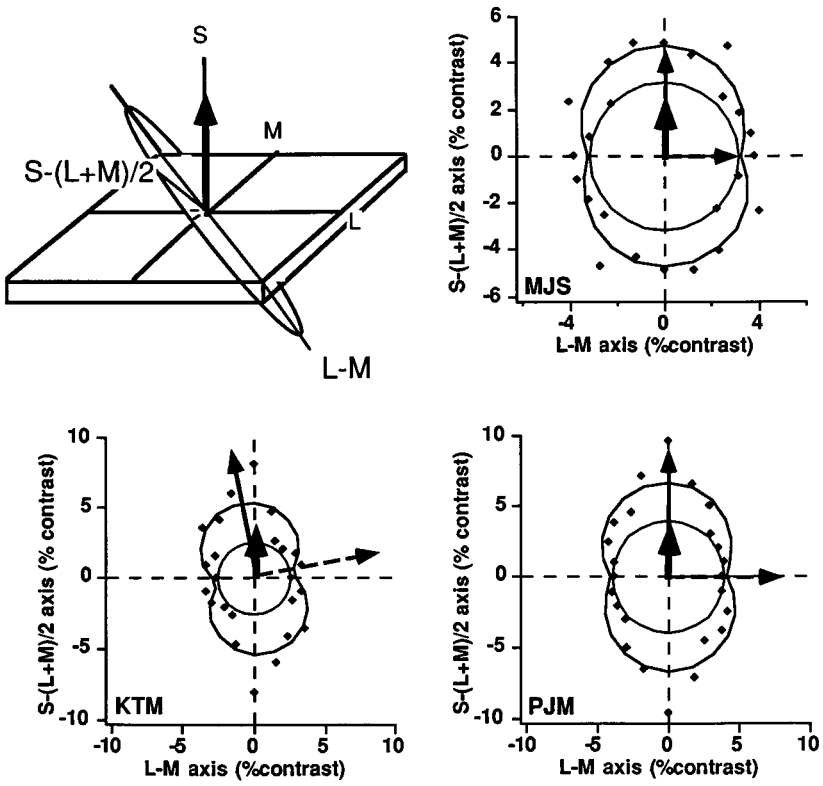

Fig. 10. Estimation of L- and M-cone weights to the blue–yellow mechanism. See caption for Fig. 4. Variable component of noise is fixed at 10% contrast. Noise components are fixed in the L + M + S direction (10% contrast) and in the L − M direction (1.8% contrast). Maximum masking in S − (L + M)/2 direction suggests this as the cone input weights to this mechanism.

blue–yellow cardinal direction, the noise plane was chosen as that orthogonal to the luminance cardinal direction. In this plane the cone contrasts all sum to zero. From our previous result for the blue–yellow signal in the by/lum noise plane, we observed that the S-cone input to the blue–yellow mechanism was balanced by the combined L- and M-cone inputs. Thus we know that the blue–yellow mechanism lies close to the chosen noise plane. Second, we introduced noise (C_n = 10%) orthogonal to this plane, i.e., in the luminance cardinal direction, in order to mask the luminance mechanism without affecting the other two mechanisms. Third, we introduced a fixed component of low-contrast noise (C_n = 1.8%) in the L−M direction to mask the red–green mechanism and thus better reveal the blue–yellow mechanism. Finally, we removed the Gaussian envelope of the noise for subjects MJS and PJM to maximize the power spectral density of the noise. The QUEST procedure was used for subjects MJS and PJM.

These results are shown in Fig. 10. The axes of the noise plane are the L − M and S − (L + M)/2 axes. For the three subjects the mechanism projection, given by the direction of maximum masking from the best cosine fit, is close to the S − (L + M)/2 direction. Given that the mechanism direction is known to be close to the noise plane, this result suggests that the mechanism direction, and therefore the associated cone weight, is given by S − (L + M)/2, i.e., an S-cone input balanced by an additive combination of equally weighted L and M cones.

4. DISCUSSION

Our noise-masking data in 3D cone contrast space supports the existence of no more than three postreceptoral mechanisms. For each of three signal directions placed in and intermediate to the cardinal directions, the nulls of noise masking lay in the other cardinal directions and not orthogonal to the signal. This demonstrated that the nulls were not determined directly by the signal but by the detection of the signal by a single underlying mechanism lying in one of the three postulated directions. This result differs from those of Gegenfurtner and Kiper,[6] where the underlying mechanisms were found always to lie in the signal direction. We have furthermore observed that a signal fixed in a direction intermediate to the cardinal directions still produced nulls in cardinal directions. This demonstrates that even intermediate signals are detected by one or more of the three purported mechanisms. This finding is enhanced by independent reports from all three subjects that the appearance of the intermediate signal varied from that of red–green, when the noise was near luminance, to that of luminance, when the noise was near red–green. This result is consistent with a recent study on target/background segmentation using related techniques.[35] The existence of only three mechanisms is consistent with the results of some adaptation studies,[2] although others have suggested the presence of intermediate mechanisms, perhaps at a higher level than those used for detection tasks.[3,4] The presence

of only three mechanisms is also consistent with a probability summation model of detection threshold contours.[12] Our results also concur with the physiological pooling of macaque lateral geniculate nucleus cells.[36]

Our measurements in addition support the choices of the cone weights to our postulated mechanisms. These cone weights agree with previous estimates from detection contours[11,12,14,15,21] and with the measurements of Derrington *et al.*[36] in macaque lateral geniculate nucleus. We were furthermore able to use our noise-masking technique to estimate the relative L- and M-cone weights to the blue–yellow mechanism—an estimate that is difficult to obtain, owing to the relatively extremely high sensitivity of the red–green mechanism. We estimated that the blue–yellow mechanism has L- and M-cone weights roughly equal to each other, in accordance with the Noorlander–Koenderink[11] model of detection thresholds and the Derrington *et al.*[36] physiology in macaque.

In a control experiment we observed the independence of the three selected cardinal directions. This was revealed by the absence of masking of a signal in any one cardinal direction by noise placed in any other. We in fact obtained facilitation of red–green signal detection by luminance noise, so far observed only for masking by gratings[20,37] or spots,[38] and facilitation of blue–yellow detection by red–green noise for both subjects. Our finding of mechanism independence further supports the presence of only three mechanisms, assuming that detection mechanisms consist of linear combinations of three cone types. With three mechanisms, each independent cardinal direction is determined as the unique normal direction to the other two mechanisms. For each mechanism of a four-mechanism model, no cardinal direction can be found in three dimensions that is orthogonal to the other three mechanism directions. Independent cardinal directions in other higher-level tasks (e.g., adaptation[2] and visual search[39]) may be found at higher levels of visual processing following nonlinear combination of the postreceptoral mechanisms. The results of our study, however, indicate that detection, even in the presence of noise, is subserved by mechanisms combining cone inputs linearly. Our observation of the independence of the cardinal directions agrees with similar measurements of noise-masking functions[5,6,20,37] but not with the Gur and Akri[22] measurements of frequency-of-seeing functions. Independence for all three cardinal directions was also observed in the Krauskopf *et al.*[2] adaptation experiments. Mechanism independence is also consistent with models of probability summation for detection contours.[12,21,40]

Our results differ from results of a similar study by Gegenfurtner and Kiper.[6] For all our conditions the positions of the nulls suggested that detection was subserved by our postulated set of three mechanisms, and in many cases the cosine model was obeyed. In the results of Gegenfurtner and Kiper, the nulls were always orthogonal to the signal direction, and the cosine model was never obeyed. We consider here possible explanations for this discrepancy. First, we believe that the color representation is critical to the interpretation of the results. Gegenfurtner and Kiper plotted their results in a space in which the cardinal directions were represented by orthogonal axes. In our study the cardinal axes were not orthogonal. Instead, we used a cone-based representation in which models of signal detection in noise, such as the cosine model, could be directly applied. We therefore replotted their data in cone contrast space, using information provided by the authors[41] (Fig. 11). These replots are compared with a near replication of their chromatic tuning measurements by subject MJS (Fig. 12). We note first that, following the transformation of the data of Gegenfurtner and Kiper to cone contrast space, the nulls are not orthogonal to the signal direction. This is contrary to their result derived from their cardinal-based representation of the same data. It is clear, therefore, that interpretation of their data is critically dependent on the representation. Furthermore, the new tuning functions from both the replot and the replication produce nulls near our chosen cardinal directions for all signals. This supports the hypothesis that signal detection is subserved in this plane by only two mechanisms (red–green and luminance). In addition, only in the luminance condition of the replication was the cosine model obeyed. This re-

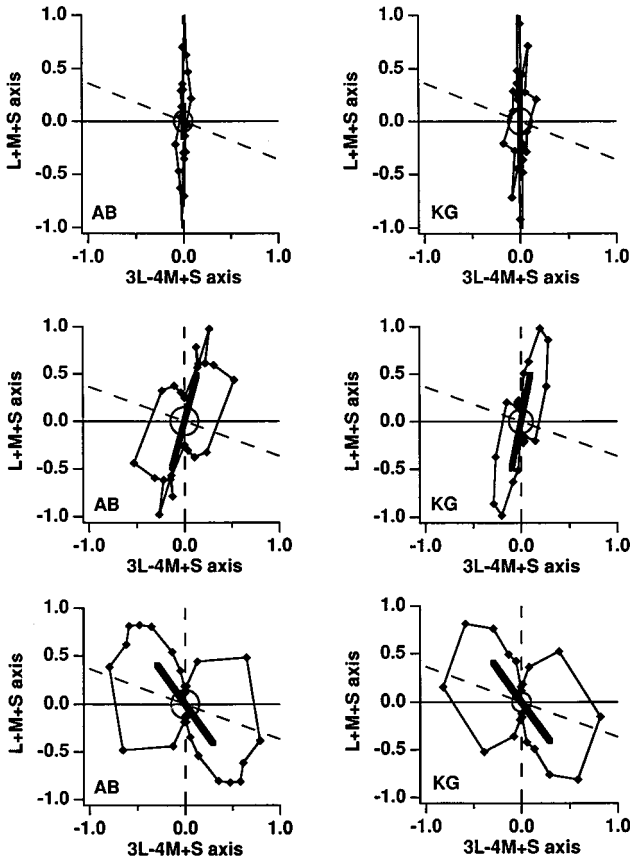

Fig. 11. Replot in cone contrast space of results from Gegenfurtner and Kiper[6]: replot of results for subjects AB and KG in Fig. 6 of that study, using calibration information provided by the authors. Signal contrast threshold (diamonds) shown as function of noise direction in cone contrast space for luminance (upper panels), intermediate (middle panels), and red–green (lower panels) signals (signal direction is denoted by thick bars). Minimum contrast threshold is predicted by the three-mechanism model to lie along one or more of the cardinal axes (dashed lines: vertical = luminance; sloping = red–green). Nulls appear to lie in cardinal directions, in agreement with the three-mechanism model.

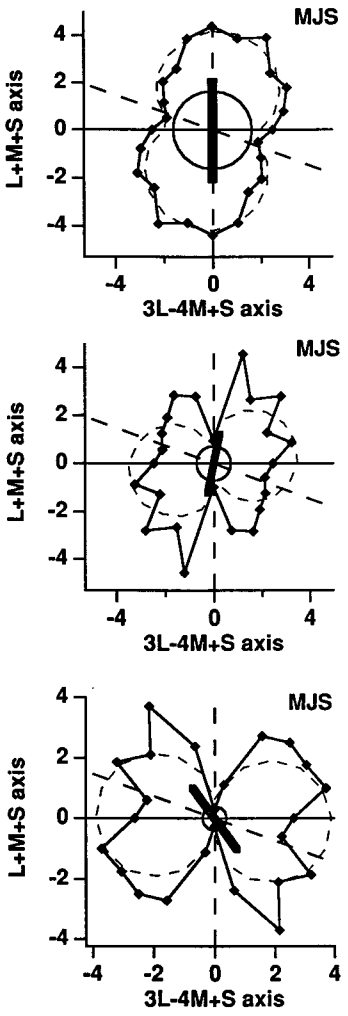

Fig. 12. Replication of results from Gegenfurtner and Kiper[6]: results for subject MJS in our study replicating the method for results shown in Fig. 11. See caption for Fig. 11. Thin dashed curve represents the fit to the cosine model. Differences between Fig. 11 and 12 are due mainly to differing constraints on the contrast of noise as its direction varied (see text). The cosine model is obeyed only for the luminance signal. The nominal red–green signal (thick arrow, bottom panel) does not lie in our proposed cardinal direction (sloping dashed line).

flects the requirement for the cosine model that the signal be detected by only a single mechanism. This is not the case for Gegenfurtner and Kiper's choice of red–green cardinal direction, which differs from ours (Fig. 12).

We also note that only in the luminance condition do the replot and the replication differ. The discrepancy in the luminance condition probably reflects a significant difference between their method and that of our replication. In each condition, Gegenfurtner and Kiper held the noise contrast constant as normalized to the luminance and red–green thresholds of each subject. In our replication, noise contrast was held constant in cone contrast space, as is necessary for the direct application of the cosine model. Because luminance threshold is four times greater than that for red–green in cone contrast space, Gegenfurtner and Kiper's tuning function would tend to be elongated along the luminance axis. This elongation would be especially significant for the luminance signal, whose tuning function is already elongated toward the luminance axis. This effect could potentially account for the difference between the replot and the replication for the luminance signal. However, attempts to compensate for it by using the model of Eq. 4 were inconclusive in verifying this.

Other major differences between the replot and the replication were that we used one-dimensional (1D) spatially and temporally low-passed noise, whereas Gegenfurtner and Kiper used two-dimensional (2D) spatiotemporally broadband noise. Differences do exist between the magnitudes of 1D and 2D masking[42] and their use of broadband noise may introduce chromatic aberration. These differences, however, would not explain the discrepancy. The difference may be caused by higher-level differences between 1D and 2D noise, such as an improved ability to segregate a 1D luminance signal from 2D, as opposed to 1D, noise. Further experiments measuring the effects of spatial variations of signal and noise would be necessary to test this possibility.

5. CONCLUSION

Our noise-masking experiments support the existence of only three postreceptoral mechanisms—two chromatic (red–green and blue–yellow) and one achromatic (luminance). This conclusion is derived from two results. First, by fixing the signal in each of the three cardinal directions, we obtained chromatic tuning functions that obeyed the linear cosine model and yielded masking nulls in the other cardinal directions. Second, the observed independence of signal and noise fixed in the three cardinal directions requires the existence of no more than three mechanisms, assuming that the mechanisms are linear combinations of the three cone types. Finally, we have established that the interpretation of chromatic tuning functions depends critically on the chosen color space and that cone contrast space is particularly suitable, assuming that detection mechanisms consist of linear combination of cone inputs.

ACKNOWLEDGMENTS

We thank Angeles Losada for her constructive comments. This study was supported by a grant from the Medical Research Council of Canada (MT-10819).

The authors can be reached at the address on the title page or by tel: 514-842-1231, ext: 4763; fax: 514-843-1691; or e-mail: sanco@violet.vision.mcgill.ca.

REFERENCES AND NOTES

1. K. Kranda and P. E. King-Smith, "Detection of coloured stimuli by independent linear systems," Vision Res. **19**, 733–745 (1979).
2. J. Krauskopf, D. R. Williams, and D. W. Heeley, "Cardinal directions of colour space," Vision Res. **22**, 1123–1131 (1982).
3. J. Krauskopf, D. R. Williams, M. B. Mandler, and A. M. Brown, "Higher order color mechanisms," Vision Res. **26**, 23–32 (1986).
4. J. Krauskopf and K. Gegenfurtner, "Color discrimination and adaptation," Vision Res. **32**, 2165–2175 (1992).

5. M. D'Zmura, "Surface color psychophysics," Ph.D. dissertation (University of Rochester, Rochester, N.Y., 1990).
6. K. R. Gegenfurtner and D. C. Kiper, "Contrast detection in luminance and chromatic noise," J. Opt. Soc. Am. A **9**, 1880–1888 (1992).
7. F. Giulianini and R. T. Eskew, Jr., "Noise masking of chromatic and achromatic detection mechanisms," Invest. Ophthalmol. Visual Sci. Suppl. **36**, 663 (1995).
8. F. Giulianini, W. Lee, and R. T. Eskew, Jr., "Chromatic noise masking of gabor patches in contrast space," Invest. Ophthalmol. Visual Sci. Suppl. **37**, 427 (1996).
9. H. G. Sperling and R. S. Harwerth, "Red-green cone interactions in the increment threshold spectral sensitivity of primates," Science **172**, 180–184 (1971).
10. B. A. Wandell, "Color measurement and discrimination," J. Opt. Soc. Am. A **2**, 62–71 (1985).
11. C. Noorlander and J. J. Koenderink, "Spatial and temporal discrimination ellipsoids in color space," J. Opt. Soc. Am. **73**, 1533–1543 (1983).
12. G. R. Cole, T. Hine, and W. McIlhagga, "Detection mechanisms in L-, M-, and S-cone contrast space," J. Opt. Soc. Am. A **10**, 38–51 (1993).
13. R. F. Quick, "A vector-magnitude model for contrast detection," Kybernetic **16**, 65–67 (1974).
14. C. F. Stromeyer III, G. R. Cole, and R. E. Kronauer, "Second-site adaptation in the red–green chromatic pathways," Vision Res. **25**, 219–237 (1985).
15. M. J. Sankeralli and K. T. Mullen, "Estimation of the L-, M-, and S-cone weights of the postreceptoral detection mechanisms," J. Opt. Soc. Am. A **13**, 906–915 (1996).
16. C. F. Stromeyer III, R. E. Kronauer, A. Ryu, A. Chaparro, and R. T. Eskew, Jr., "Contributions of human long-wave and middle-wave cones to motion detection," J. Physiol. (London) **485**, 211–243 (1995).
17. A. B. Poirson, B. A. Wandell, D. C. Varner, and D. H. Brainard, "Surface characterizations of color thresholds," J. Opt. Soc. Am. A **7**, 783–789 (1990).
18. G. R. Cole, T. J. Hine, and W. McIlhagga, "Estimation of linear detection mechanisms for stimuli of medium spatial frequency," Vision Res. **34**, 1267–1278 (1994).
19. K. Knoblauch and L. T. Maloney, "Testing the indeterminacy of linear color mechanisms from color discrimination data," Vision Res. **36**, 295–306 (1996).
20. K. T. Mullen and M. A. Losada, "Evidence for separate pathways for color and luminance detection mechanisms," J. Opt. Soc. Am. A **11**, 3136–3151 (1994).
21. A. B. Metha, A. J. Vingrys, and D. R. Badcock, "Detection and discrimination of moving stimuli: the effects of color, luminance, and eccentricity," J. Opt. Soc. Am. A **11**, 1697–1709 (1994).
22. M. Gur and V. Akri, "Isoluminant stimuli may not expose the full contribution of color to visual functioning: spatial contrast sensitivity measurements indicate interaction between color and luminance processing," Vision Res. **32**, 1253–1262 (1992).
23. W. P. Tanner, Jr., and T. G. Birdsall, "Definitions of d' and h as psychometric measures," J. Acoust. Soc. Am. **30**, 922–928 (1958).
24. D. M. Green and J. A. Swets, *Signal Detection Theory and Psychophysics* (Wiley, New York, 1966).
25. D. G. Pelli, "The effects of visual noise," Ph.D. dissertation (Cambridge University, Cambridge, 1981).
26. A. E. Burgess, R. F. Wagner, R. J. Jennings, and H. B. Barlow, "Efficiency of human visual signal discrimination," Science **214**, 93–94 (1981).
27. D. G. Pelli and L. Zhang, "Accurate control of contrast on microcomputer displays," Vision Res. **31**, 1337–1350 (1991).
28. W. H. Press, S. A. Teukolsky, W. T. Vetterling, and B. P. Flannery, *Numerical Recipes in C: The Art of Scientific Computing*, 2nd ed. (Cambridge U. Press, Cambridge, 1992).
29. D. I. Flitcroft, "The interactions between chromatic aberration, defocus and stimulus chromaticity: implications for visual physiology and colorimetry," Vision Res. **29**, 349–360 (1989).
30. A. Bradley, L. Zhang, and L. N. Thibos, "Failures of isoluminance caused by ocular chromatic aberration," Appl. Opt. **31**, 3657–3667 (1992).
31. A. V. Oppenheim and R. W. Schafer, *Discrete-Time Signal Processing* (Prentice-Hall, Englewood Cliffs, N.J., 1989).
32. D. I. A. Macleod and R. M. Boynton, "Chromaticity diagram showing cone excitation by stimuli by equal luminance," J. Opt. Soc. Am. **69**, 1183–1186 (1979).
33. A. B. Watson and D. G. Pelli, "QUEST: a Bayesian adaptive psychometric method," Percept. Psychophys. **33**, 113–120 (1983).
34. A. Chaparro, R. Thabet, C. F. Stromeyer III, and R. E. Kronauer, "Spatial masking: mechanisms jointly tuned to color and luminance?" Invest. Ophthalmol. Visual Sci. Suppl. **37**, 3 (1996).
35. A. Li and P. Lennie, "Mechanisms underlying segmentation of colored textures," Vision Res. **37**, 83–97 (1997).
36. A. M. Derrington, J. Krauskopf, and P. Lennie, "Chromatic mechanisms in lateral geniculate nucleus of macaque," J. Physiol. (London) **357**, 241–265 (1984).
37. E. Switkes, A. Bradley, and K. K. De Valois, "Contrast dependence and mechanisms of masking interactions among chromatic and luminance gratings," J. Opt. Soc. Am. A **5**, 1149–1162 (1988).
38. G. R. Cole, C. F. Stromeyer, and R. E. Kronauer, "Visual interactions with luminance and chromatic stimuli," J. Opt. Soc. Am. A **7**, 128–140 (1990).
39. M. D'Zmura, "Color in visual search," Vision Res. **13**, 951–966 (1991).
40. K. T. Mullen, S. J. Cropper, and M. A. Losada, "Absence of linear subthreshold summation between red–green and luminance mechanisms over a wide range of spatio-temporal conditions," Vision Res. **37**, 1157–1165 (1997).
41. CIE coordinates provided were as follows: mean white point, (0.32, 0.33); one unit on red axis, (0.337, 0.323); one unit on green axis, (0.303, 0.339); one unit on luminance axis, 0.138 contrast unit. These were converted to cone excitations with the CIE/Smith–Pokorny conversion equations [see P. K. Kaiser and R. M. Boynton, *Human Color Vision*, 2nd ed. (Optical Society of America, Washington D.C., 1996), p. 557] and then to cone contrast units by normalizing by the cone excitations at the mean white point. In our (r, θ, ϕ) cone contrast representation, Gegenfurtner and Kiper's[6] luminance and red–green axes were found, respectively, to be (45°, 35.3°), as in our study, and (83.0°, 21.6°), differing somewhat from ours. Using these two axes, we converted intermediate directions by linear transforms.
42. J. Rovamo and H. Kukkonen, "The effect of noise check size and shape on grating delectability," Vision Res. **36**, 271–279 (1996).